NV5 GEOSPATIAL
powered by QUANTUM SPATIAL

March 30, 2021
Revision 1: July 16, 2021

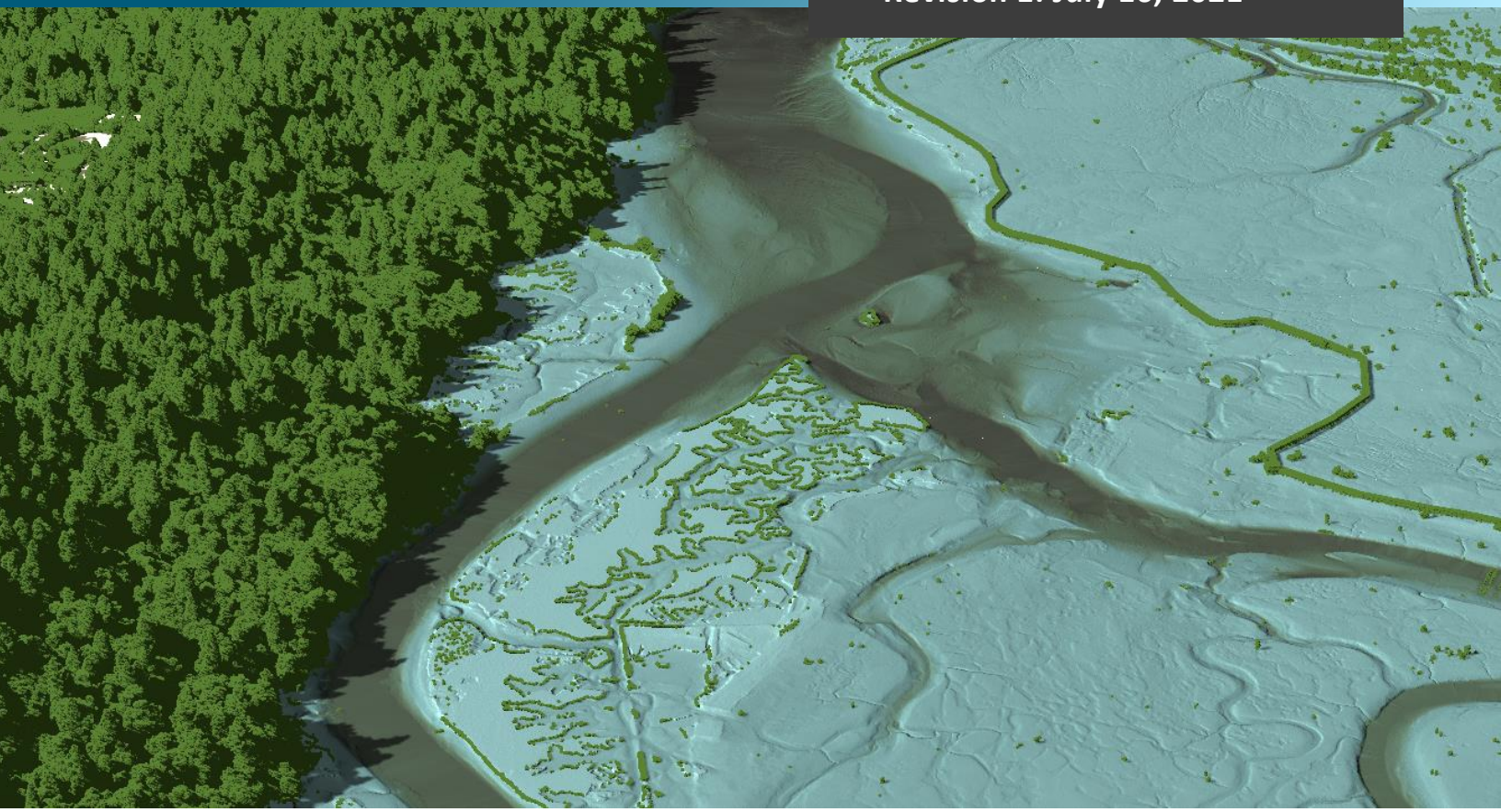

Nisqually River Basin, Washington Topobathymetric Lidar Technical Data Report

Task Order: 140G0220F0241
Work Package ID: 198224

Contract: G16PC00016
Work Unit ID: 198221

Prepared For:

USGS
science for a changing world

United States Geological Survey
Robert Hasselwander
1400 Independence Road
Rolla, MO 65401
PH: 573-308-3642

Prepared By:

NV5 GEOSPATIAL
powered by QUANTUM SPATIAL

NV5 Geospatial Corvallis
1100 NE Circle Blvd, Ste. 126
Corvallis, OR 97330
PH: 541-752-1204

TABLE OF CONTENTS

Cover Photo: A view looking north over the Nisqually Estuary in the Nisqually National Wildlife Refuge. The image was created from the lidar bare earth model, overlayed with the above-ground point cloud, and colored by elevation.

INTRODUCTION

This photo taken by NV5 acquisition staff shows a view of the Nisqually Estuary boardwalk in the northern section of the Nisqually River Basin site in Washington.

In September 2020, NV5 Geospatial (NV5) was contracted by the United States Geologic Survey (USGS) to collect topobathymetric Light Detection and Ranging (lidar) data in the winter of 2020 for the Nisqually River Basin site in Washington. The Nisqually River Basin project area covers roughly 21 square miles near the Nisqually Reservation. Traditional near-infrared (NIR) lidar was fully integrated with green wavelength return data (bathymetric) lidar in order to provide a seamless topobathymetric lidar dataset. Data were collected to aid USGS and the Nisqually Indian Tribe in conservation planning, research, delivery, floodplain mapping, and hydrologic modeling, and the 3DEP mission.

This report accompanies the delivered topobathymetric lidar data, and documents contract specifications, data acquisition procedures, processing methods, and analysis of the final dataset including lidar accuracy, and density. Acquisition dates and acreage are shown in Table 1, a complete list of contracted deliverables provided to USGS is shown in Table 2, and the project extent is shown in Figure 1.

Table 1: Acquisition dates, acreage, and data types collected on the Nisqually River Basin site

Project Site	Contracted Acres	Buffered Acres	Acquisition Dates	Data Type
Nisqually River Basin, Washington	12,147	13,189	11/08/2020 & 12/22/2020	Topobathymetric Lidar

Deliverable Products

Table 2: Products delivered to USGS for the Nisqually River Basin site

Nisqually River Basin Topobathymetric Lidar Products Projection: UTM Zone 10 North Horizontal Datum: NAD83 (2011) Vertical Datum: NAVD88 (GEOID18) Units: Meters	
Topobathymetric Lidar	
Points	LAS v 1.4 • All Classified Returns
Rasters	1.0 Meter GeoTiffs • Bare Earth Digital Elevation Model – Hydroflattened and Bridge Enforced (DEM) • Topobathymetric Bare Earth Digital Elevation Mode – Clipped to Void and Bridge Enforced (DEM) • Highest Hit Digital Surface Model (DSM) • Height Separation Rasters 0.5 Meter GeoTiffs • Green Sensor Intensity Image Tiles • NIR Sensor Intensity Image Tiles
Vectors	ESRI file geodatabase • Project Boundary • Tile Index • 2D Hydro-Breaklines • 3D Hydroflattened-Breaklines • Bridge Breaklines • Ground Survey Shapes • Flightline Index • Flightline Swath Coverage Extents

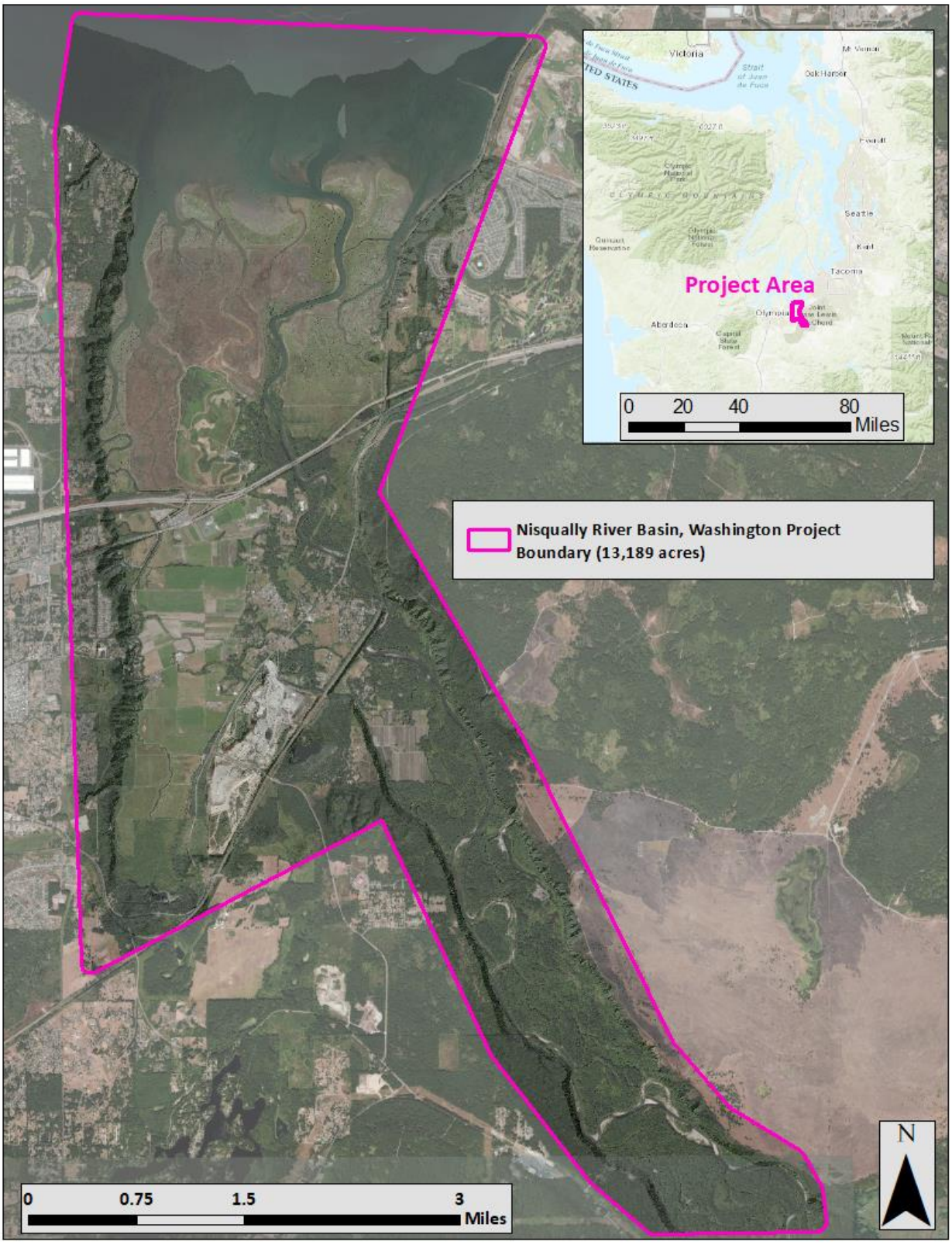

Figure 1: Location map of the Nisqually River Basin site in Washington

ACQUISITION

NV5's ground acquisition equipment set up in the Nisqually River Basin Topobathametric Lidar area near Hogum Bay.

Planning

In preparation for data collection, NV5 reviewed the project area and developed a specialized flight plan to ensure complete coverage of the Nisqually River Basin Lidar study area at the target combined point density of ≥15 points/m^2. Acquisition parameters including orientation relative to terrain, flight altitude, pulse rate, scan angle, and ground speed were adapted to optimize flight paths and flight times while meeting all contract specifications.

Factors such as satellite constellation availability and weather windows must be considered during the planning stage. Any weather hazards or conditions affecting the flight were continuously monitored due to their potential impact on the daily success of airborne and ground operations. In addition, logistical considerations including private property access, potential air space restrictions, channel flow rates, tides (Figure 3 and Figure 4), and water clarity were reviewed.

Turbidity Measurements and Secchi Depth Readings

In order to assess water clarity conditions prior to and during lidar and digital imagery collection, NV5 collected turbidity measurements, and secchi depth readings at 5 locations throughout the project site between September 21st and November 13th, 2020. Turbidity and wind observations were recorded twice to confirm measurements. NV5's ground survey team used a Sper Scientific 860040 Turbidity Meter and a standard 20 cm diameter, black and white secchi disk attached to a rope to collect turbidity readings within the project site. Table 3 below provides turbidity and secchi depth results per site on each day of data collection. A map of turbidity reading locations and secchi depth sites is provided as Figure 2.

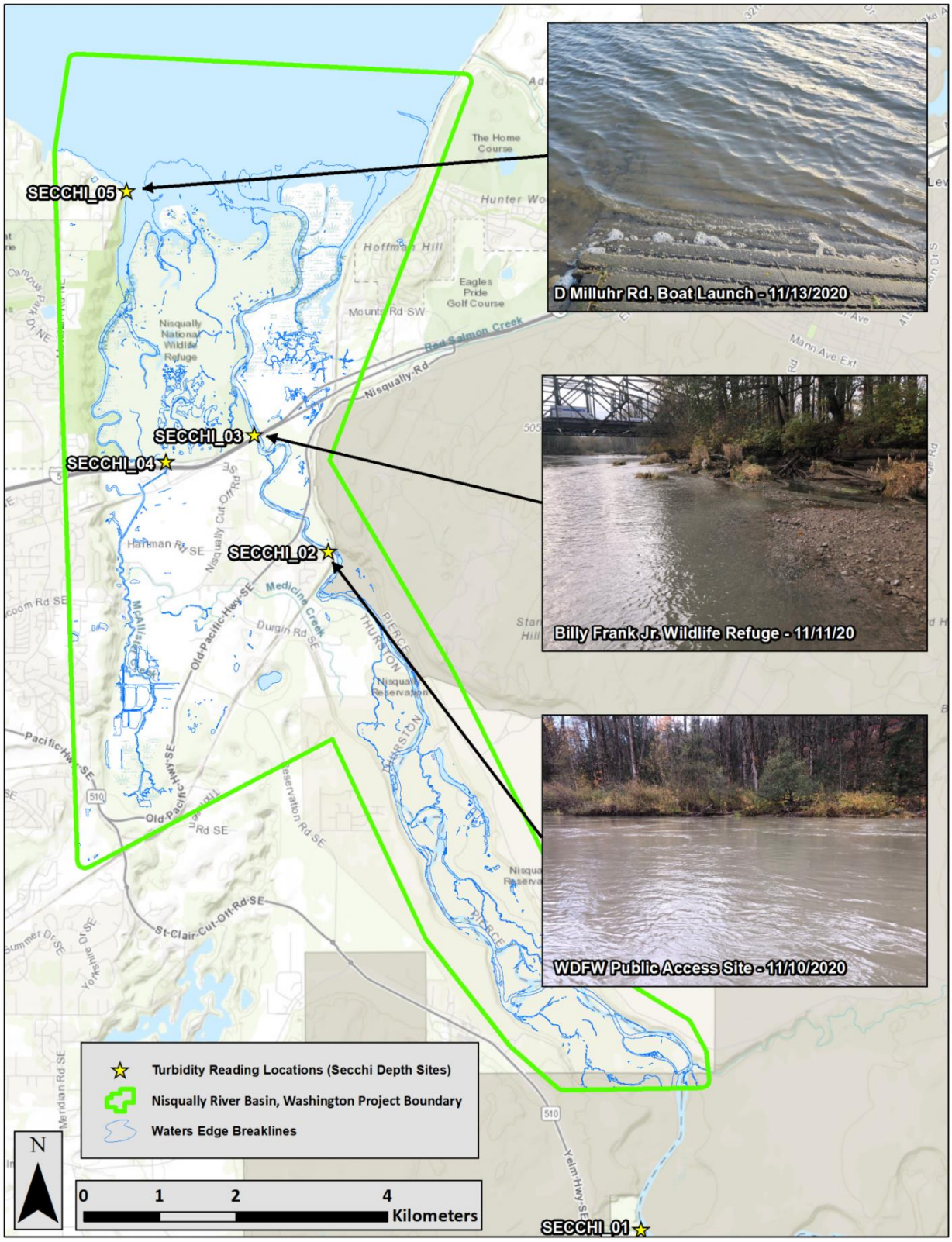

Figure 2: Turbidity Reading Locations (Secchi Depth Sites)

Sper Scientific 860040 Turbidity Meter

20 cm diameter, black and white secchi disk attached to rope

Table 3: Water Clarity Observations for Lidar flights

Turbidity, Secchi Depth, and Wind Speed Observations								
Date	**Location**	**Secchi ID**	**Longitude**	**Latitude**	**Turbidity Read 1 NTU**	**Turbidity Read 2 NTU**	**Turbidity Read 3 NTU**	***Secchi Depth (m)**
11/08 11:10 am	Nisqually River at Yelm Powerhouse Park	SECCHI_01	122° 38’ 17.60” W	46°58’38.81”N	25.89	25.26	25.32	0.36
11/08 4:25 pm	Nisqually River at Yelm Powerhouse Park	SECCHI_01	122° 38’ 17.60” W	46°58’38.81”N	27.54	27.85	27.74	0.28
09/21 4:30 pm	Nisqually River Public Access Site	SECCHI_02	122° 41’ 30.96” W	47° 3’ 28.96”N	7.50	n/a	n/a	0.75
11/08 12:55 pm	Nisqually River Public Access Site	SECCHI_02	122° 41’ 30.96” W	47° 3’ 28.96”N	21.27	20.70	22.22	0.35
11/08 3:55 pm	Nisqually River Public Access Site	SECCHI_02	122° 41’ 30.96” W	47° 3’ 28.96”N	23.67	24.00	23.69	0.33
11/10 1:25 pm	Nisqually River Public Access Site	SECCHI_02	122° 41’ 30.96” W	47° 3’ 28.96”N	19.35	19.91	19.81	0.36
11/08 2:15 pm	Billy Frank Jr. Wildlife Refuge	SECCHI_03	122° 42’ 17.06” W	47° 4’ 18.91”N	21.59	21.36	21.85	0.33
11/08 3:25 pm	Billy Frank Jr. Wildlife Refuge	SECCHI_03	122° 42’ 17.06” W	47° 4’ 18.91”N	22.64	23.62	22.91	0.29
11/11 8:35 am	Billy Frank Jr. Wildlife Refuge	SECCHI_03	122° 42’ 17.06” W	47° 4’ 18.91”N	14.09	14.26	13.95	0.40
11/08 2:50 pm	MCallister Creek	SECCHI_04	122° 43’ 12.16” W	47° 4’ 7.54” N	4.77	4.95	4.99	0.93
11/11 10:15 am	MCallister Creek	SECCHI_04	122° 43’ 12.16” W	47° 4’ 7.54” N	3.68	3.79	4.03	0.97
11/13 9:15 am	D Milluhr Rd. Boat Launch	SECCHI_05	122° 43’ 36.35” W	47° 6’ 3.24” N	2.81	2.67	2.63	Bottom: 1.00

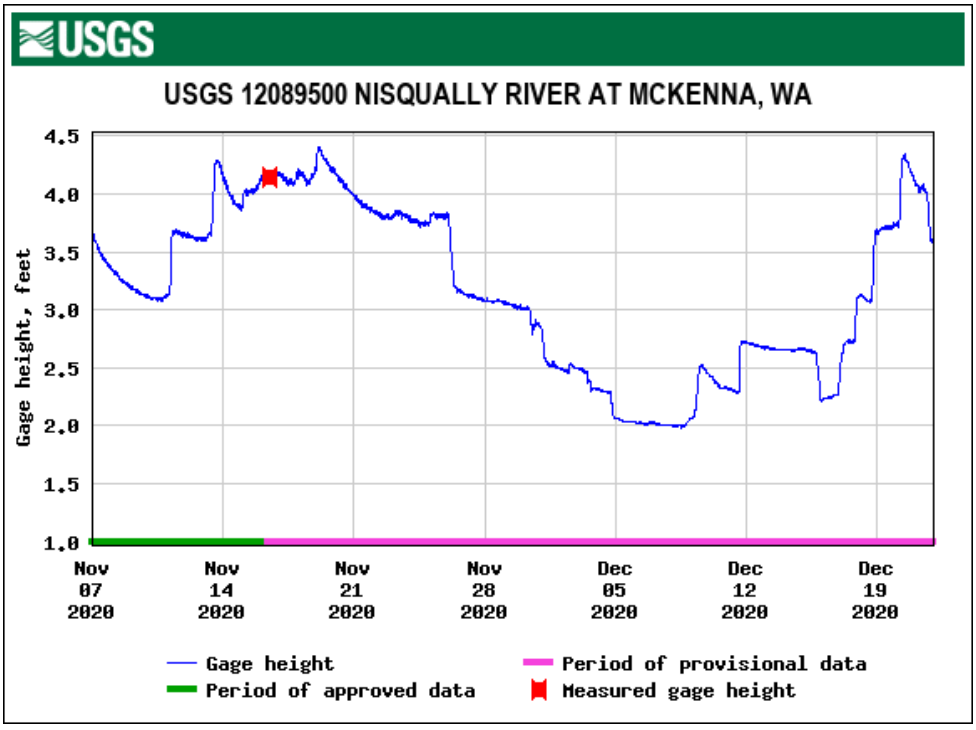

Figure 3: USGS Station 12089500 gage height along the Nisqually River at the time of lidar acquisition.

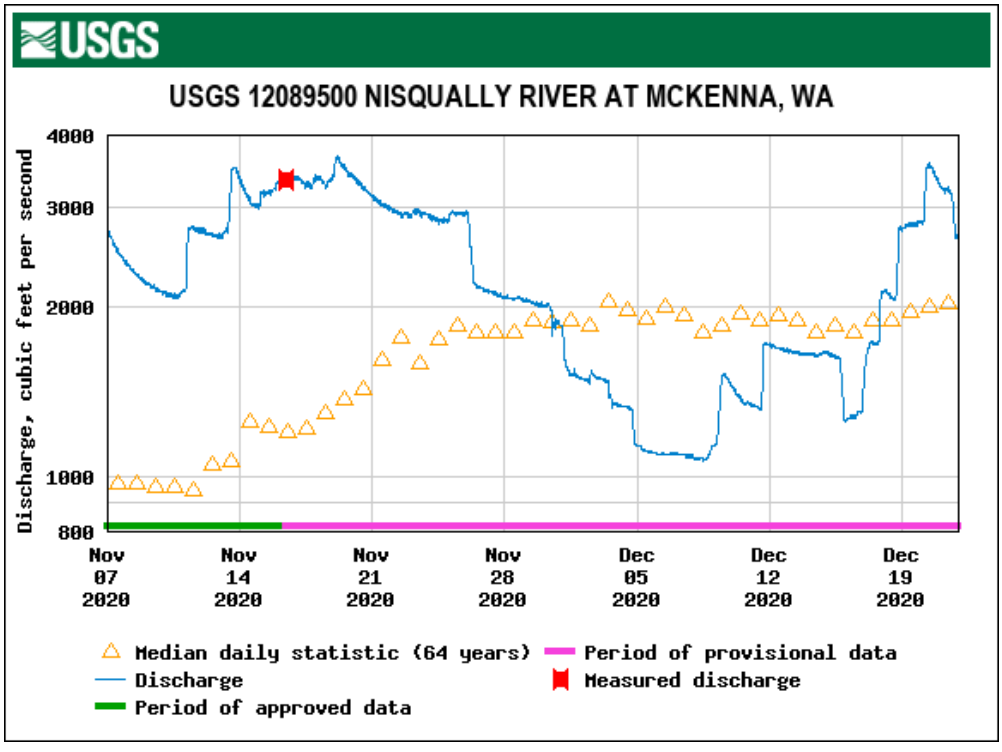

Figure 4: USGS Station 12089500 flow rates along the Nisqually River at the time of lidar acquisition.

These photos taken by NV5 acquisition staff display water clarity conditions within the Nisqually River Basin site.

Airborne Lidar Survey

The lidar survey was accomplished using a Riegl VQ-880-GII green laser system mounted in a Cessna Caravan (Table 4). The Riegl VQ-880-GII boasts a higher repetition pulse rate (up to 550 kHz), higher scanning speed, small laser footprint, and wide field of view which allows for seamless collection of high resolution data of both topographic and bathymetric surfaces. The green wavelength (ʎ=532 nm) laser is capable of collecting high resolution topography data, as well as penetrating the water surface with minimal spectral absorption by water. The Riegl VQ-880-GII contains an integrated NIR laser (ʎ=1064 nm) that adds additional topography data and aids in water surface modeling. The recorded waveform enables range measurements for all discernible targets for a given pulse. The typical number of returns digitized from a single pulse range from 1 to 15 for the Nisqually River Basin project area. It is not uncommon for some types of surfaces (e.g., dense vegetation or water) to return fewer pulses to the lidar sensor than the laser originally emitted. The discrepancy between first return and overall delivered density will vary depending on terrain, land cover, and the prevalence of water bodies. All discernible laser returns were processed for the output dataset. Table 5 summarizes the settings used to yield an average pulse density of ≥15 pulses/m^2 over the Nisqually River Basin project area.

Table 4: Flight Date Table

Date	Flight Line #	Start Time (Adjsted GPS)	End Time (Adjusted GPS)
11/08/2020	400-453, 30400-30431, 30432-30453	288869791.763	288879530.561
12/22/2020	300-357, 30300-30357	292691074.656	292702391.547

Table 5: Lidar specifications and survey settings

Lidar Survey Settings & Specifications		
Acquisition Dates	11/08/2020 & 12/22/2020	11/08/2020 & 12/22/2020
Aircraft Used	Cessna Caravan	Cessna Caravan
Sensor	Riegl	Riegl
Laser	VQ-880-GII	VQ-880GII-IR
Maximum Returns	15	15
Resolution/Density	Average 15 pulses/m^2	Average 15 pulses/m^2
Nominal Pulse Spacing	0.26 m	0.26 m
Survey Altitude (AGL)	400 m	400 m
Survey speed	140 knots	140 knots
Field of View	40°	42°
Mirror Scan Rate	66.3 Hz	Uniform Point Spacing
Target Pulse Rate	245 kHz	145 kHz
Pulse Length	1.5 ns	3 ns
Laser Pulse Footprint Diameter	28.0 cm	8.0 cm
Central Wavelength	532 nm	1,064 nm
Pulse Mode	Multiple Times Around (MTA)	Multiple Times Around (MTA)
Beam Divergence	0.7 mrad	0.2 mrad
Swath Width	291 m	307 m
Swath Overlap	60%	60%
Intensity	16-bit	16-bit
Accuracy	$RMSE_Z \leq 15$ cm	$RMSE_Z \leq 15$ cm

All areas were surveyed with an opposing flight line side-lap of ≥50% (≥100% overlap) in order to reduce laser shadowing and increase surface laser painting. To accurately solve for laser point position (geographic coordinates x, y and z), the positional coordinates of the airborne sensor and the attitude of the aircraft were recorded continuously throughout the lidar data collection mission. Position of the aircraft was measured twice per second (2 Hz) by an onboard differential GPS unit, and aircraft attitude was measured 200 times per second (200 Hz) as pitch, roll and yaw (heading) from an onboard inertial measurement unit (IMU). To allow for post-processing correction and calibration, aircraft and sensor position and attitude data are indexed by GPS time.

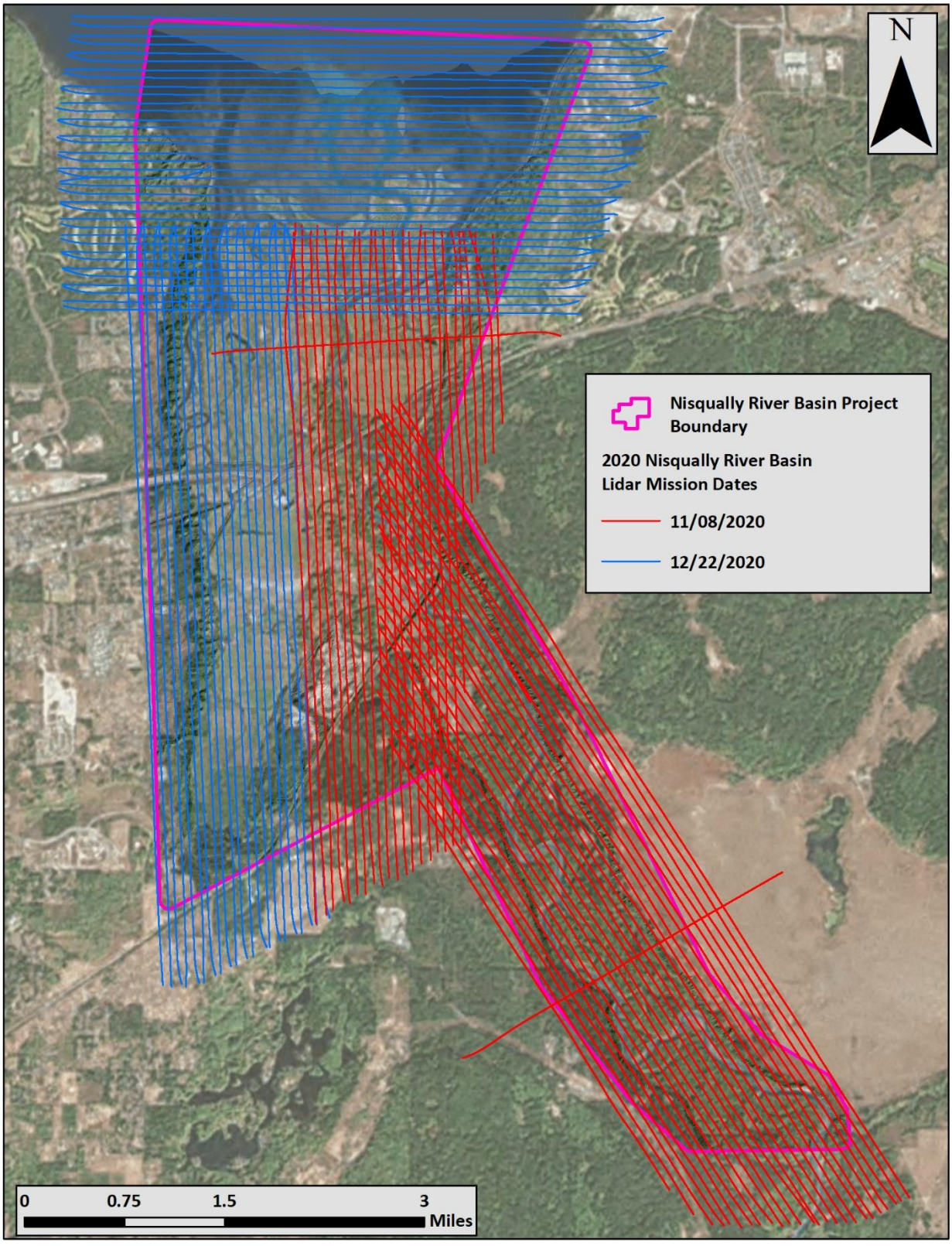

Figure 5: 2020 Aerial Acquisition Flightline Map

Ground Survey

Ground control surveys, including monumentation and ground survey points (GSPs), were conducted to support the airborne acquisition. Ground control data were used to geospatially correct the aircraft positional coordinate data and to perform quality assurance checks on final lidar data.

NV5's survey equipment over a FWS Monument in the Nisqually National Wilife Refuge

Base Stations

Monuments were used for collection of ground survey points using real time kinematic (RTK) , post processed kinematic (PPK), and Total station (TS) survey techniques.

Base station locations were selected with consideration for satellite visibility, field crew safety, and optimal location for GSP coverage. NV5 utilized two permanent active base stations from the Washington State Reference Network (WSRN), one base station from the Smartnet GNSS Real-Time Network (RTN), and one existing US FWS monument for the Nisqually River Basin lidar acquisition (Table 6, Figure 6). FWS_Nisqually coordinates were provided by the client referenced to NAD83(CORS96) and transformed to NAD83(2011) by NV5. NV5's professional land surveyor, Evon Silvia (WAPLS#53957) oversaw and certified the occupation of all base stations.

Table 6: Monument positions for the Nisqually River Basin acquisition. Coordinates are on the NAD83 (2011) datum, epoch 2010.00

Monument ID	Owner	Latitude	Longitude	Ellipsoid (meters)
FWS_Nisqually	US FWS	47° 04' 24.89661"	122° 42' 52.72080"	-18.266
OLAR	WSRN	46° 57' 40.28899"	122° 54' 30.41255"	41.391
OLMP	WSRN	47° 02' 41.43490"	122° 53' 42.72317"	2.933
WAOL	SmartNet	47° 02' 47.31394"	122° 50' 37.49367"	45.749

NV5 utilized static Global Navigation Satellite System (GNSS) data collected at 1 Hz recording frequency for each base station. During post-processing, the static GNSS data was triangulated with nearby Continuously Operating Reference Stations (CORS) using the Online Positioning User Service (OPUS[1]) for precise positioning. Multiple independent sessions over the same monument were processed to confirm antenna height measurements and to refine position accuracy.

[1] OPUS is a free service provided by the National Geodetic Survey to process corrected monument positions. http://www.ngs.noaa.gov/OPUS/.

Monuments were established according to the national standard for geodetic control networks, as specified in the Federal Geographic Data Committee (FGDC) Geospatial Positioning Accuracy Standards for geodetic networks.[2] This standard provides guidelines for classification of monument quality at the 95% confidence interval as a basis for comparing the quality of one control network to another. The monument rating for this project is shown in Table 7.

Table 7: Federal Geographic Data Committee monument rating for network accuracy

Direction	Rating
1.96 * St Dev $_{NE}$:	0.020 m
1.96 * St Dev $_{z}$:	0.020 m

For the Nisqually River Basin Lidar project, the monument coordinates contributed no more than 2.8 cm of positional error to the geolocation of the final ground survey points and lidar, with 95% confidence.

[2] Federal Geographic Data Committee, Geospatial Positioning Accuracy Standards (FGDC-STD-007.2-1998). Part 2: Standards for Geodetic Networks, Table 2.1, page 2-3. http://www.fgdc.gov/standards/projects/FGDC-standards-projects/accuracy/part2/chapter2

Ground Survey Points (GSPs)

Ground survey points were collected using real time kinematic (RTK), post-processed kinematic (PPK), and total station (TS) survey techniques. For RTK surveys, a roving receiver receives corrections from a nearby base station or Real-Time Network (RTN) via radio or cellular network, enabling rapid collection of points with relative errors less than 1.5 cm horizontal and 2.0 cm vertical. PPK surveys compute these corrections during post-processing to achieve comparable accuracy. RTK and PPK surveys record data while stationary for at least five seconds, calculating the position using at least three one-second epochs. All GSP measurements were made during periods with a Position Dilution of Precision (PDOP) of ≤ 3.0 with at least six satellites in view of the stationary and roving receivers. See Table 8 for NV5 ground survey equipment information.

Forested check points were collected using a total station in order to measure positions under dense canopy. Total staion backsight and setup points were established using RTK survey techniques with long occupation times.

GSPs were collected in areas where good satellite visibility was achieved on paved roads and other hard surfaces such as gravel or packed dirt roads. GSP measurements were not taken on highly reflective surfaces such as center line stripes or lane markings on roads due to the increased noise seen in the laser returns over these surfaces. GSPs were collected within as many flightlines as possible; however, the distribution of GSPs depended on ground access constraints and monument locations and may not be equitably distributed throughout the study area (Figure 6).

Table 8: NV5 ground survey equipment identification

Receiver Model	Antenna	OPUS Antenna ID	Use
Trimble R7	Zephyr GNSS Geodetic Model 2 RoHS	TRM57971.00	Static
Trimble R10 Model 2	Integrated Antenna	TRMR10-2	Rover
Nikon NPL-322+5” P		n/a	Total Station

Land Cover Class

In addition to ground survey points, land cover class check points were collected throughout the study area to evaluate vertical accuracy. Vertical accuracy statistics were calculated for all land cover types to assess confidence in the lidar derived ground models across land cover classes (Table 9, see Lidar Accuracy Assessments, page 29).

Table 9: Land Cover Types and Descriptions

Land cover type	Land cover code	Example	Description	Accuracy Assessment Type
Shrub	SH		Areas dominated by lowland brush and woody vegetation	VVA
Tall Grass	TG		Herbaceous grasslands in advanced stages of growth	VVA
Forest	FR		Forested areas	VVA
Bare Earth	BE		Areas of bare earth surface	NVA
Urban	UA		Areas dominated by urban development, including parks	NVA

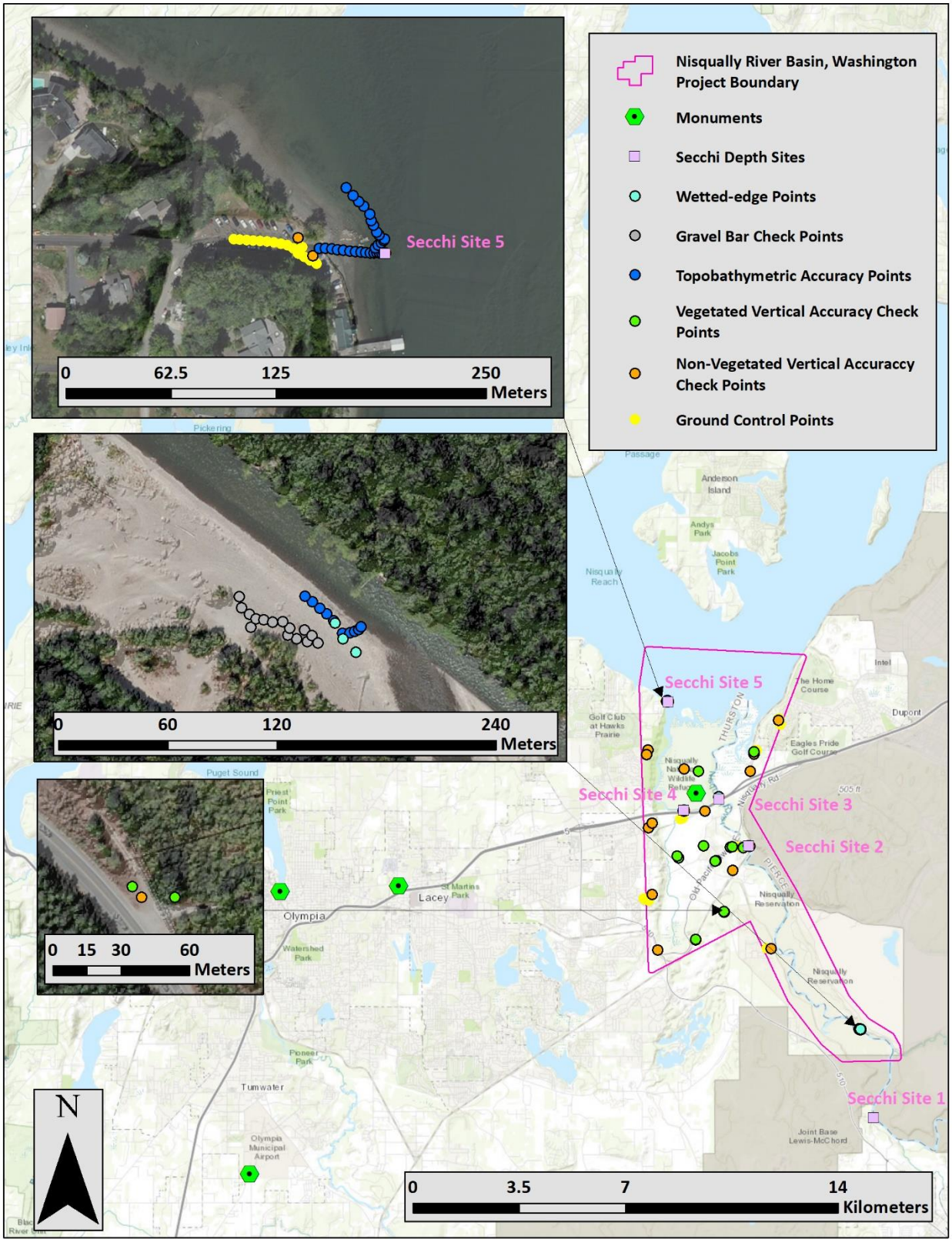

Figure 6: Ground survey location map

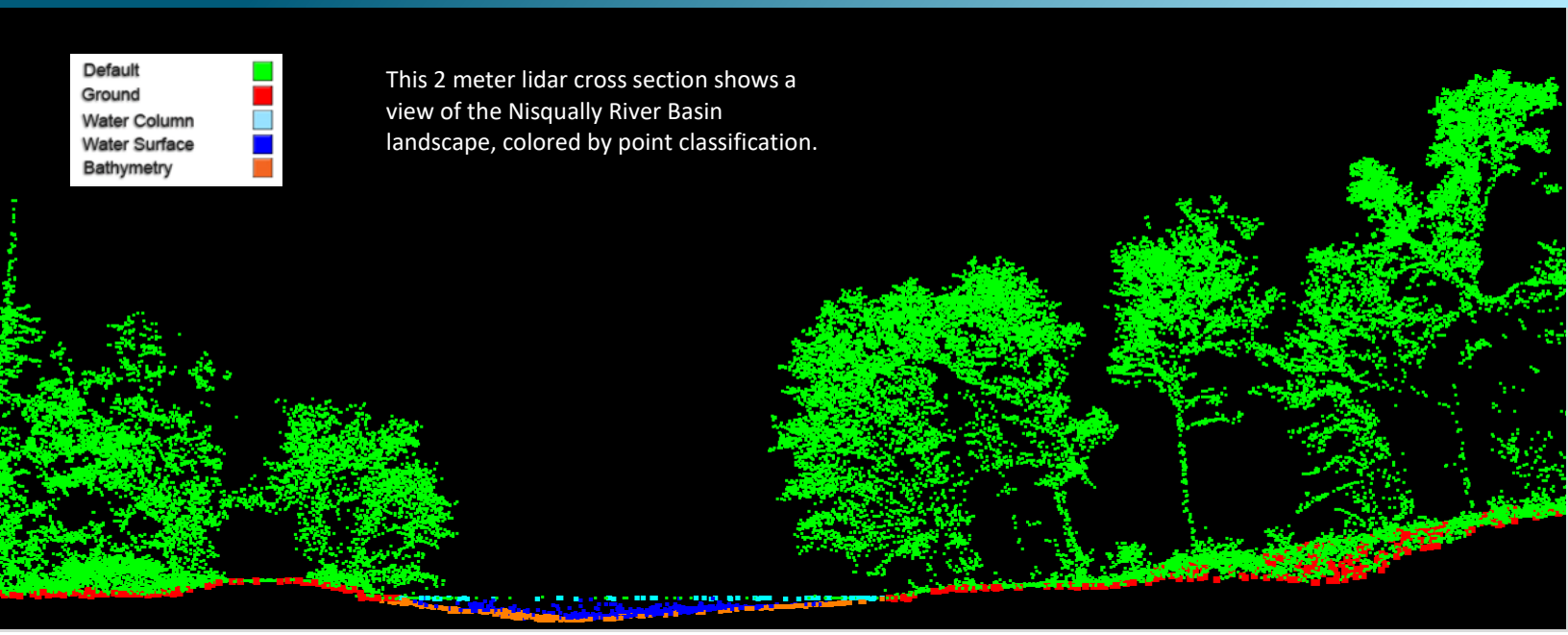

This 2 meter lidar cross section shows a view of the Nisqually River Basin landscape, colored by point classification.

Topobathymetric Lidar Data

Upon completion of data acquisition, NV5 processing staff initiated a suite of automated and manual techniques to process the data into the requested deliverables. Processing tasks included GPS control computations, smoothed best estimate trajectory (SBET) calculations, kinematic corrections, calculation of laser point position, sensor and data calibration for optimal relative and absolute accuracy, and lidar point classification (Table 10).

Riegl's RiProcess software was used to facilitate bathymetric return processing. Once bathymetric points were differentiated, they were spatially corrected for refraction through the water column based on the angle of incidence of the laser. NV5 refracted water column points using NV5's proprietary LAS processing software, Las Monkey. The resulting point cloud data was classified using both manual and automated techniques. Processing methodologies were tailored for the landscape. Brief descriptions of these tasks are shown in Table 11 .

Table 10: ASPRS LAS classification standards applied to the Nisqually River Basin dataset

Classification Number	Classification Name	Classification Description
1	Default/Unclassified	Laser returns that are not included in the ground class, composed of vegetation and anthropogenic features
1-W	Edge Clip	Laser returns at the outer edges of flightlines that are geometrically unreliable
2	Ground	Laser returns that are determined to be ground using automated and manual cleaning algorithms
7-W	Noise	Laser returns that are often associated with artificial points below the ground surface
9	Water	Laser returns that are determined to be water using automated and manual cleaning algorithms
17	Bridge	Bridge decks
18-W	High Noise	Laser Returns that are often associated with birds and scattering from reflective surfaces
22	Temporal Exclusion	Laser returns that are determined to be due to temporal differences in flight lines and are excluded
40	Bathymetric Bottom	Refracted Riegl sensor returns that fall within the water's edge breakline which characterize the submerged topography
41	Water Surface	Green laser returns that are determined to be water surface points using automated and manual cleaning algorithms
45	Water Column	Refracted Riegl sensor returns that are determined to be water using automated and manual cleaning algorithms

Table 11: Lidar processing workflow

Lidar Processing Step	Software Used
Resolve kinematic corrections for aircraft position data using kinematic aircraft GPS and static ground GPS data. Develop a smoothed best estimate of trajectory (SBET) file that blends post-processed aircraft position with sensor head position and attitude recorded throughout the survey.	POSPac MMS v.8.5
Calculate laser point position by associating SBET position to each laser point return time, scan angle, intensity, etc. Create raw laser point cloud data for the entire survey in *.las (ASPRS v. 1.4) format. Convert data to orthometric elevations by applying a geoid correction.	POSPac MMS v.8.5 RiProcess v1.8.5 TerraMatch v.19.002
Import raw laser points into manageable blocks to perform manual relative accuracy calibration and filter erroneous points. Classify ground points for individual flight lines.	TerraScan v.19.005
Using ground classified points per each flight line, test the relative accuracy. Perform automated line-to-line calibrations for system attitude parameters (pitch, roll, heading), mirror flex (scale) and GPS/IMU drift. Calculate calibrations on ground classified points from paired flight lines and apply results to all points in a flight line. Use every flight line for relative accuracy calibration.	TerraMatch v.19.002 RiProcess v1.8.5
Apply refraction correction to all subsurface returns.	Las Monkey 2.6.2 (NV5 proprietary software)
Classify resulting data to ground and other client designated ASPRS classifications (Table 10). Assess statistical absolute accuracy via direct comparisons of ground classified points to ground control survey data.	TerraScan v.19.005 TerraModeler v.19.002
Generate bare earth models as triangulated surfaces. Generate highest hit models as a surface expression of all classified points. Export all surface models as 1.0 meter Cloud Optimized GeoTiffs pixel resolution.	Las Product Creator 3.0 (NV5 proprietary software) ArcMap v. 10.3.1
Export intensity images as Cloud Optimized GeoTIFFs at a 0.5 meter pixel resolution.	Las Product Creator 3.0 (NV5 proprietary software)

Temporal Exclusion Considerations

Due to the tidally influenced nature of the project area and multi-day acquisition, tidal differences were noted in the dataset. Specifically, two water surfaces at different elevations are present in a portion of the dataset due to overlapping swaths that were acquired on different days and at a different tidal phases (Figure 7). In this circumstance, NV5 favors the swath with the lower water surface because it provides greater topographic coverage. Points belonging to the swath of higher water surface are eligible for the temporal exclusion class. It is important to consider tidal fluctuations when observing baythmetric surfaces because surface elevations will deviate according to the amount of tidal erosion or tidal deposition.

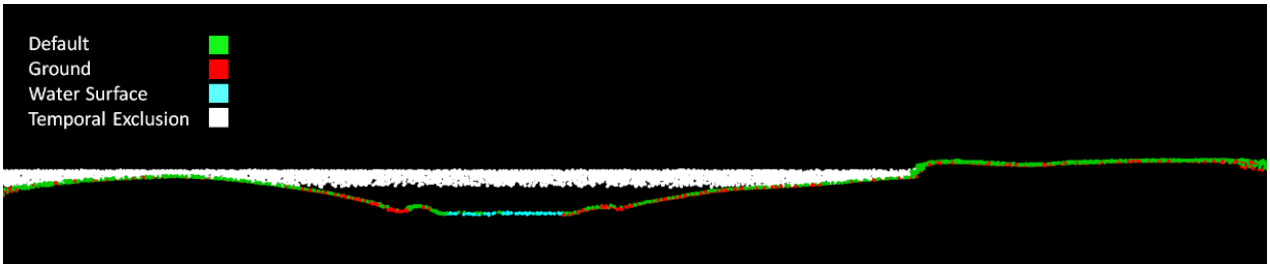

Figure 7: An example of temporal exclusion classing due to tidal changes in the Nisqually River project area. Temporal exclusion points in this 2 meter cross section represent a temporal change in water surface.

Bathymetric Refraction

Green lidar pulses that enter the water column must have their position corrected for refraction of the light beam as it passes through the water and its resulting decreased speed. NV5 has developed proprietary software (Las Monkey) to perform this processing based on Snell's law. The first step is to develop a water surface model (WSM) from the NIR lidar water surface returns.

The water surface models used for refraction are generated using elevation information derived from the NIR channel to inform where the green water surface level is located, and then water surface points are classified for both the forward and reverse look directions of the green scanner. Points are filtered and edited to obtain the most accurate representation of the water surface and are used to create a water surface model for each flight line and look direction. Water surface classification and modeling is processed on each flight line to accommodate water level changes due to tide and temporal changes in water surface. Each look direction (forward and reverse) are modeled separately to correctly model short duration time dependent surface changes (e.g. waves) that change between the times that each look direction records a unique location. The water surface model created is raster based with an associated surface normal vector to obtain the most accurate angle of incidence during refraction.

Once the WSM is generated, the Las Monkey refraction software then intersects the partially submerged green pulses with the WSM to determine the angle of incidence with the water surface and the submerged component of the pulse vector. This provides the information necessary to correct the position of underwater points by adjusting the submerged vector length and orientation. After refraction, the points are compared against bathymetric check points to assess accuracy.

Lidar Derived Products

Because hydrographic laser scanners penetrate the water surface to map submerged topography, this affects how the data should be processed and presented in derived products from the lidar point cloud. The following discusses certain derived products that vary from the traditional (NIR) specification and delivery format.

Topobathymetric DEMs

Bathymetric bottom returns can be limited by depth, water clarity, and bottom surface reflectivity. Water clarity and turbidity affects the depth penetration capability of the green wavelength laser with returning laser energy diminishing by scattering throughout the water column. Additionally, the bottom surface must be reflective enough to return remaining laser energy back to the sensor at a detectable level. Although the predicted depth penetration range of the Riegl VQ-880-GII sensor is 1.5 Secchi depths on brightly reflective surfaces, it is not unexpected to have no bathymetric bottom returns in turbid or non-reflective areas.

As a result, creating digital elevation models (DEMs) presents a challenge with respect to interpolation of areas with no returns. Traditional DEMs are “unclipped”, meaning areas lacking ground returns are interpolated from neighboring ground returns (or breaklines in the case of hydro-flattening), with the assumption that the interpolation is close to reality. In bathymetric modeling, these assumptions are prone to error because a lack of bathymetric returns can indicate a change in elevation that the laser can no longer map due to increased depths. The resulting void areas may suggest greater depths, rather than similar elevations from neighboring bathymetric bottom returns. Therefore, NV5 created a water polygon with bathymetric coverage to delineate areas with successfully mapped bathymetry. This shapefile was used to control the extent of the delivered clipped topobathymetric model to avoid false triangulation (interpolation from TIN’ing) across areas in the water with no bathymetric returns.

Intensity Images

In traditional NIR lidar, intensity images are often made using first return information. For bathymetric lidar however, it is most often the last returns that capture features of interest below the water's surface. Therefore, a first return intensity image would display intensity information of the water's surface, obscuring the features of interest below.

With bathymetric lidar a more detailed and informative intensity image can be created by using all or selected point classes, rather than relying on return number alone. If intensity information of the bathymetry is the primary goal, water surface and water column points can be excluded. However, water surface and water column points often contain potentially useful information about turbidity and submerged but unclassified features such as vegetation. For the Nisqually River Basin project, NV5 created one set of intensity images from NIR laser first returns, as well as one set of intensity images from green laser returns. Green laser intensity images were created using first returns over terrestrial areas only, as well as all water column and bathymetric bottom points in order to display more detail in intensity values (Figure 8).

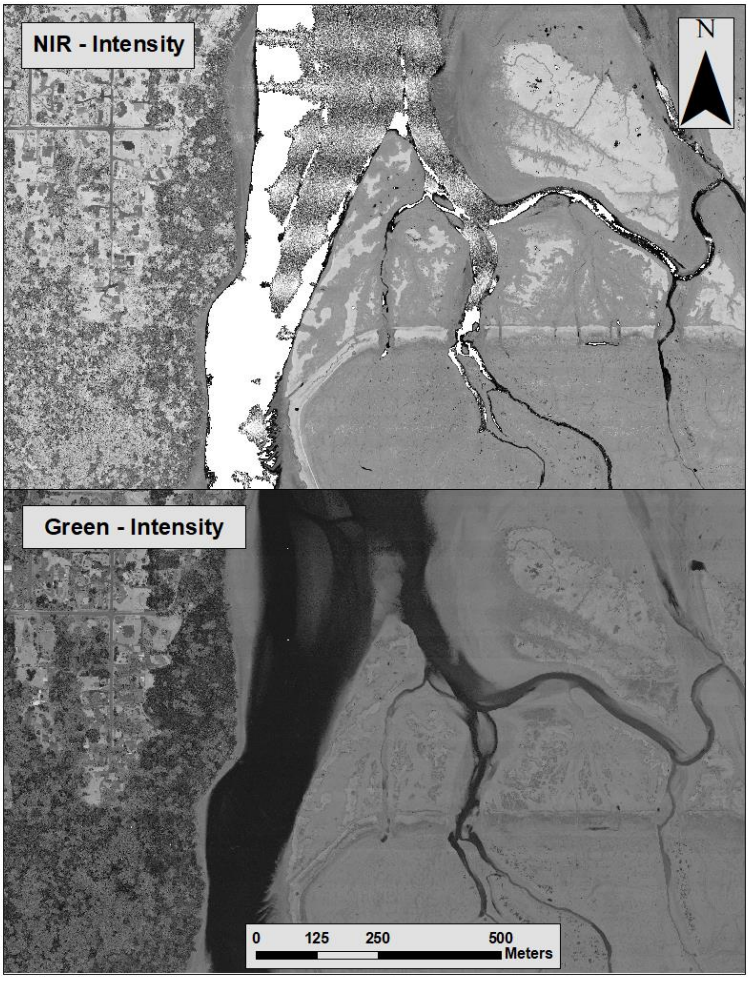

Figure 8: A comparison of Intensity Images from Green and NIR returns in the Nisqually River Basin area of interest.

Feature Extraction

Hydroflattening and Water's Edge Breaklines

The Nisqually River and other water bodies within the project area were flattened to a consistent water level. Bodies of water that were flattened include lakes and other closed water bodies with a surface area greater than 2 acres, all streams and rivers that are nominally wider than 30 meters, all tidal waters bordering the project, and select smaller bodies of water as feasible. The hydroflattening process eliminates artifacts in the digital terrain model caused by both increased variability in ranges or dropouts in laser returns due to the low reflectivity of water.

Hydroflattening of closed water bodies was performed through a combination of automated and manual detection and adjustment techniques designed to identify water boundaries and water levels. Boundary polygons were developed using an algorithm which weights lidar-derived slopes, intensities, and return densities to detect the water's edge. The water edges were then manually reviewed and edited as necessary.

Once polygons were developed the initial ground classified points falling within 1 meter outside of water polygons were reclassified as ignored ground points to omit them from the final ground model. Elevations were then obtained from the filtered lidar returns to create the final breaklines. Lakes were assigned a consistent elevation for an entire polygon while rivers were assigned consistent elevations on opposing banks and smoothed to ensure downstream flow through the entire river channel.

Water boundary breaklines were then incorporated into the hydroflattened DEM by enforcing triangle edges (adjacent to the breakline) to the elevation values of the breakline. This implementation corrected interpolation along the hard edge. Water surfaces were obtained from a TIN of the 3-D water edge breaklines resulting in the final hydroflattened model (Figure 9).

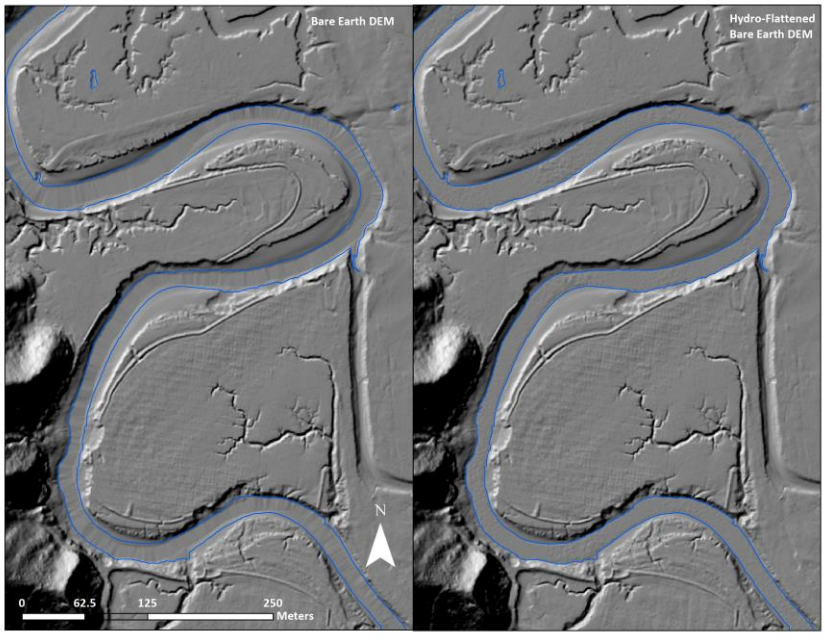

Figure 9: Example of hydroflattening in the Nisqually River Basin Lidar dataset

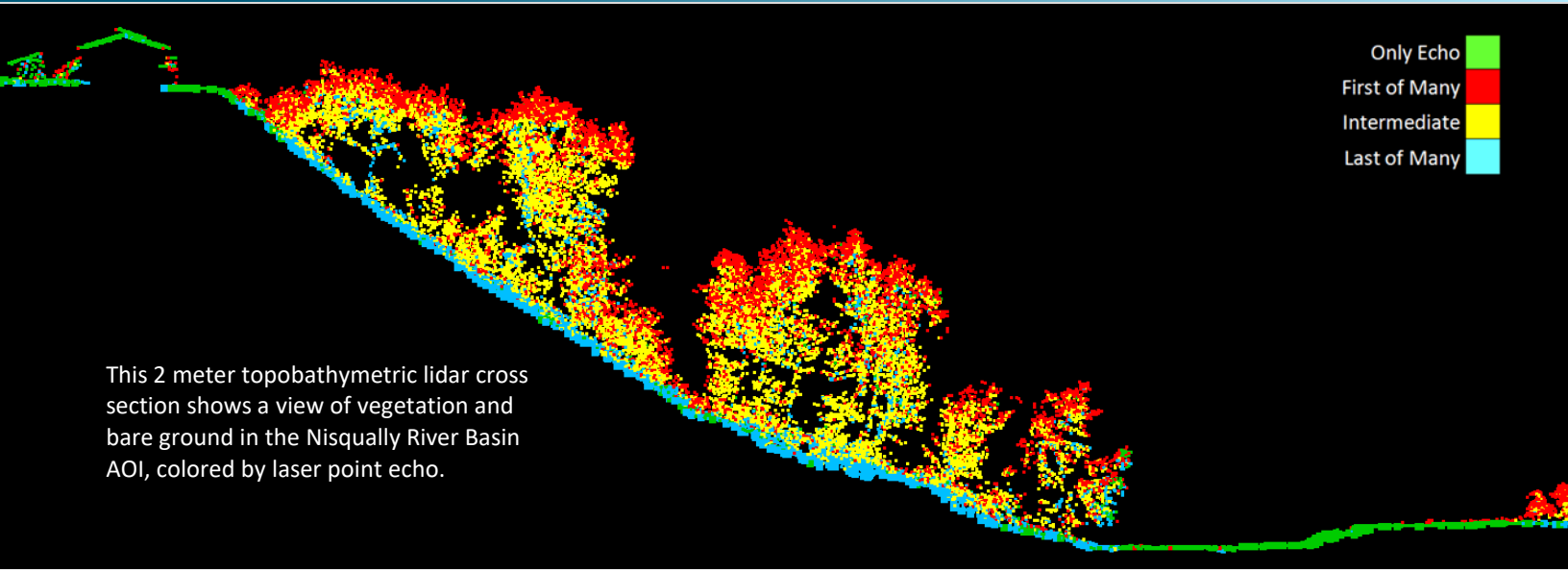

This 2 meter topobathymetric lidar cross section shows a view of vegetation and bare ground in the Nisqually River Basin AOI, colored by laser point echo.

Bathymetric Lidar

An underlying principle for collecting hydrographic lidar data is to survey near-shore areas that can be difficult to collect with other methods, such as multi-beam sonar, particularly over large areas. In order to determine the capability and effectiveness of the bathymetric lidar, several parameters were considered; depth penetrations below the water surface, bathymetric return density, and spatial accuracy.

Lidar Point Density

First Return Point Density

The acquisition parameters were designed to acquire an average first-return density of 15 points/m^2. First return density describes the density of pulses emitted from the laser that return at least one echo to the system. Multiple returns from a single pulse were not considered in first return density analysis. Some types of surfaces (e.g., breaks in terrain, water and steep slopes) may have returned fewer pulses than originally emitted by the laser.

First returns typically reflect off the highest feature on the landscape within the footprint of the pulse. In forested or urban areas the highest feature could be a tree, building or power line, while in areas of unobstructed ground, the first return will be the only echo and represents the bare earth surface.

The average first-return density of the Nisqually River Basin Lidar project was 36.59 points/m^2 (Table 12). The statistical and spatial distributions of all first return densities per 100 m x 100 m cell are portrayed in Figure 10 and Figure 12.

Bathymetric and Ground Classified Point Densities

The density of ground classified lidar returns and bathymetric bottom returns were also analyzed for this project. Terrain character, land cover, and ground surface reflectivity all influenced the density of ground surface returns. In vegetated areas, fewer pulses may have penetrated the canopy, resulting in lower ground density. Similarly, the density of bathymetric bottom returns was influenced by turbidity, depth, and bottom surface reflectivity. In turbid areas, fewer pulses may have penetrated the water surface, resulting in lower bathymetric density.

The ground and bathymetric bottom classified density of lidar data for the Nisqually River Basin project was 5.42 points/m^2(Table 12). The statistical and spatial distributions ground classified and bathymetric bottom return densities per 100 m x 100 m cell are portrayed in Figure 11 and Figure 12.

Additionally, for the Nisqually River Basin project, density values of only bathymetric bottom returns were calculated for areas containing at least one bathymetric bottom return. Areas lacking bathymetric returns (voids)were not considered in calculating an average density value. Within the successfully mapped area, a bathymetric bottom return density of 6.09 points/m^2 was achieved.

Table 12: Average Lidar point densities

Density Type	Point Density
First Returns	36.59 points/m²
Ground and Bathymetric Bottom Classified Returns	5.42 points/m²
Bathymetric Bottom Classified Returns	6.09 points/m²

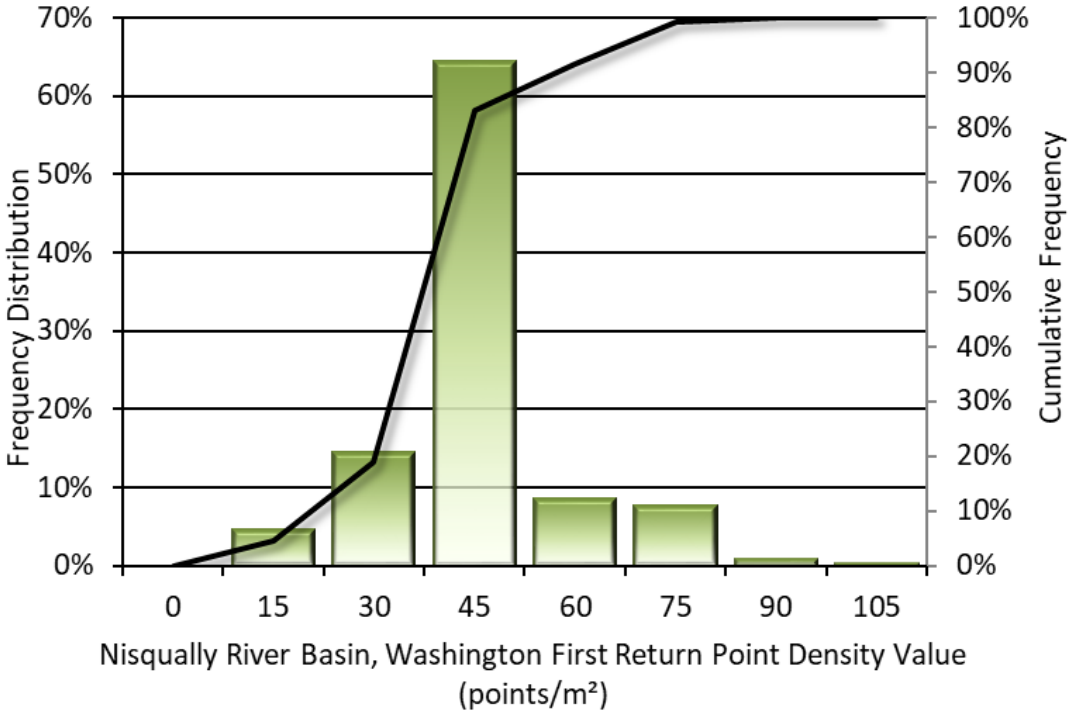

Figure 10: Frequency distribution of first return densities per 100 x 100 m cell

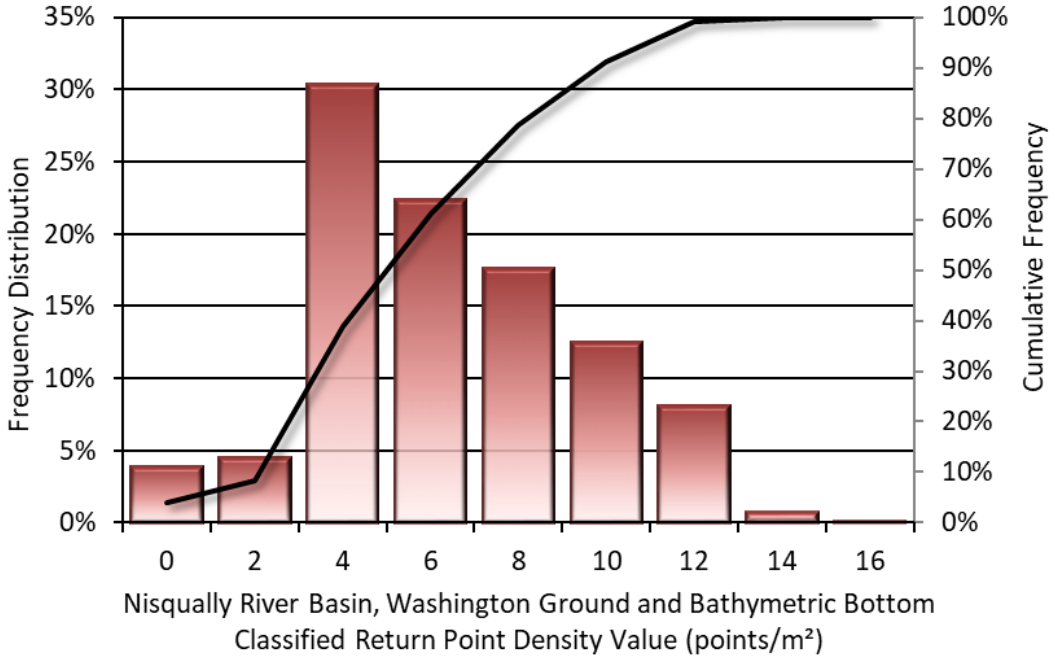

Figure 11: Frequency distribution of ground and bathymetric bottom classified return densities per 100 x 100 m cell

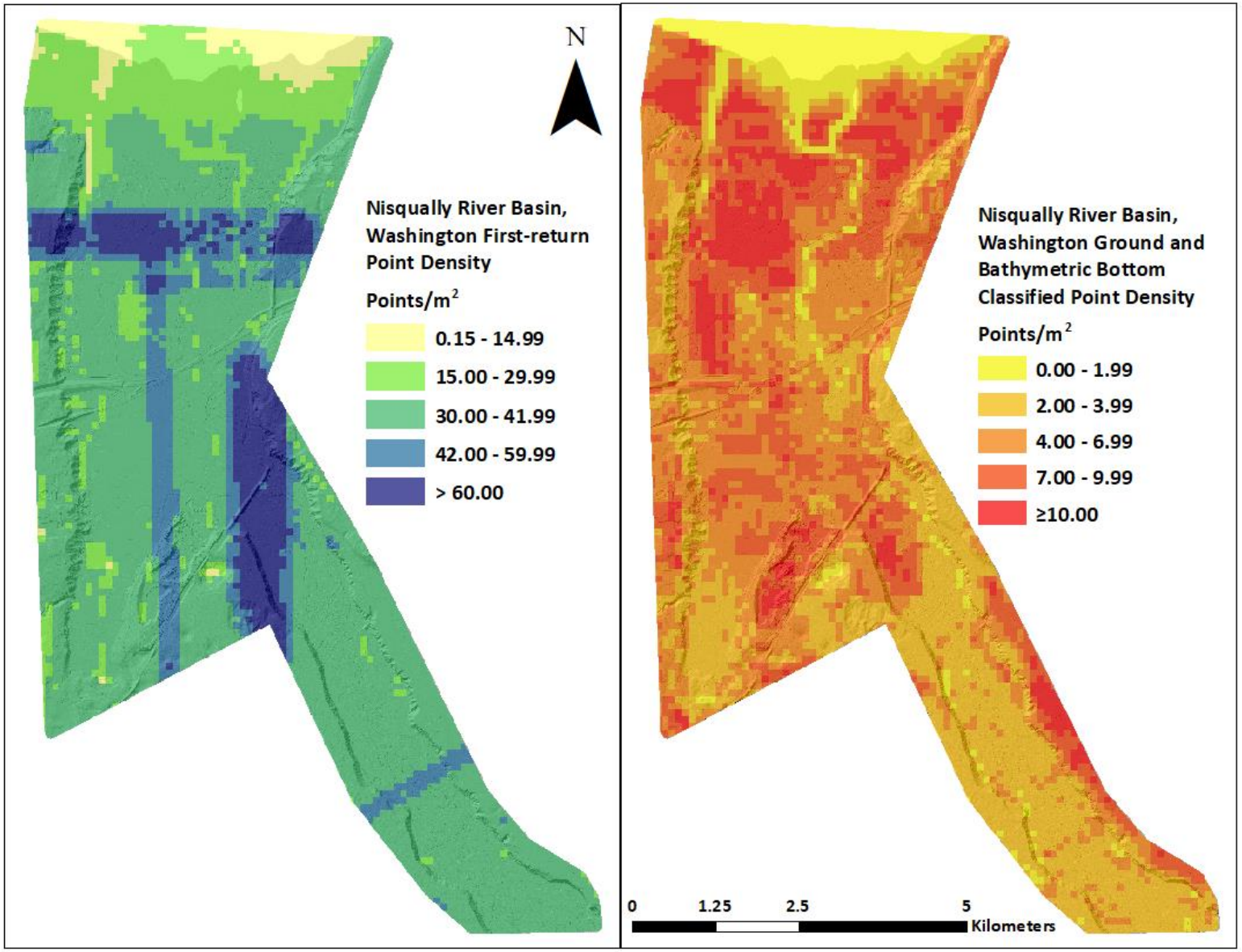

Figure 12: First return and ground and bathymetric bottom density map for the Nisqually River Basin site (100 m x 100 m cells)

Lidar Accuracy Assessments

The accuracy of the lidar data collection can be described in terms of absolute accuracy (the consistency of the data with external data sources) and relative accuracy (the consistency of the dataset with itself). See Appendix A for further information on sources of error and operational measures used to improve relative accuracy.

Lidar Non-Vegetated Vertical Accuracy

Absolute accuracy was assessed using Non-vegetated Vertical Accuracy (NVA) reporting designed to meet guidelines presented in the FGDC National Standard for Spatial Data Accuracy[3]. NVA compares known ground check point data that were withheld from the calibration and post-processing of the lidar point cloud to the triangulated surface generated by the classified lidar point cloud as well as the derived gridded bare earth DEM. NVA is a measure of the accuracy of lidar point data in open areas where the lidar system has a high probability of measuring the ground surface and is evaluated at the 95% confidence interval (1.96 * RMSE), as shown in Table 13.

The mean and standard deviation (sigma σ) of divergence of the ground surface model from ground check point coordinates are also considered during accuracy assessment. These statistics assume the error for x, y and z is normally distributed, and therefore the skew and kurtosis of distributions are also considered when evaluating error statistics. For the Nisqually River Basin survey, 22 ground check points were withheld from the calibration and post-processing of the lidar point cloud, with resulting non-vegetated vertical accuracy of 0.039 meters as compared to the classified LAS and 0.046 meters against the bare earth DEM, with 95% confidence (Figure 13 and Figure 14).

NV5 also assessed absolute accuracy using 192 ground control points. Although these points were used in the calibration and post-processing of the lidar point cloud, they still provide a good indication of the overall accuracy of the lidar dataset, and therefore have been provided in Table 13 and Figure 15.

[3] Federal Geographic Data Committee, ASPRS POSITIONAL ACCURACY STANDARDS FOR DIGITAL GEOSPATIAL DATA EDITION 1, Version 1.0, NOVEMBER 2014. https://www.asprs.org/a/society/committees/standards/Positional_Accuracy_Standards.pdf.

Table 13: Absolute accuracy results

Absolute Vertical Accuracy			
	NVA, as compared to Classified LAS	**NVA, as compared to Bare Earth DEM**	**Ground Control Points**
Sample	22 points	22 points	192 points
95% Confidence (1.96*RMSE)	0.039 m	0.046 m	0.045 m
Average	-0.011 m	-0.011 m	-0.004 m
Median	-0.009 m	-0.009 m	-0.001 m
RMSE	0.020 m	0.023 m	0.023 m
Standard Deviation (1σ)	0.017 m	0.021 m	0.023 m

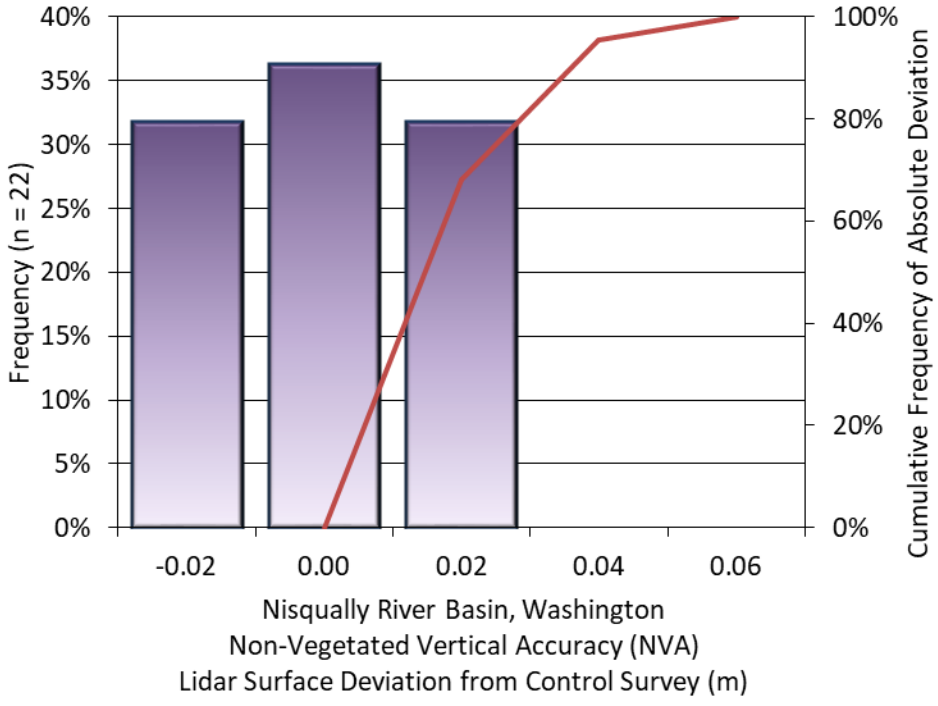

Figure 13: Frequency histogram for classified LAS deviation from ground check point values

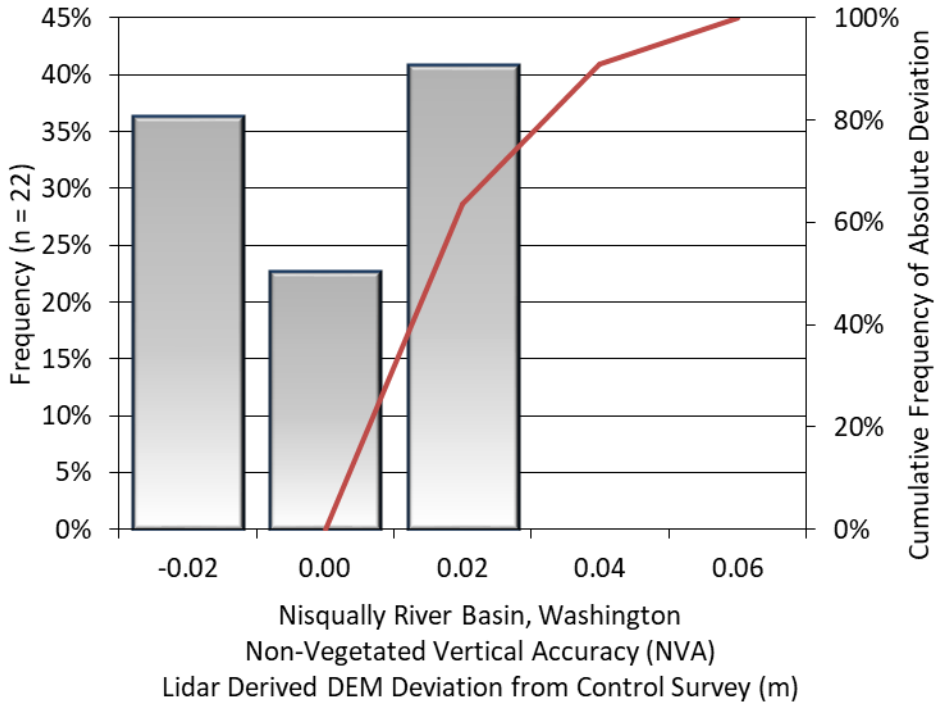

Figure 14: Frequency histogram for lidar bare earth DEM deviation from ground check point values

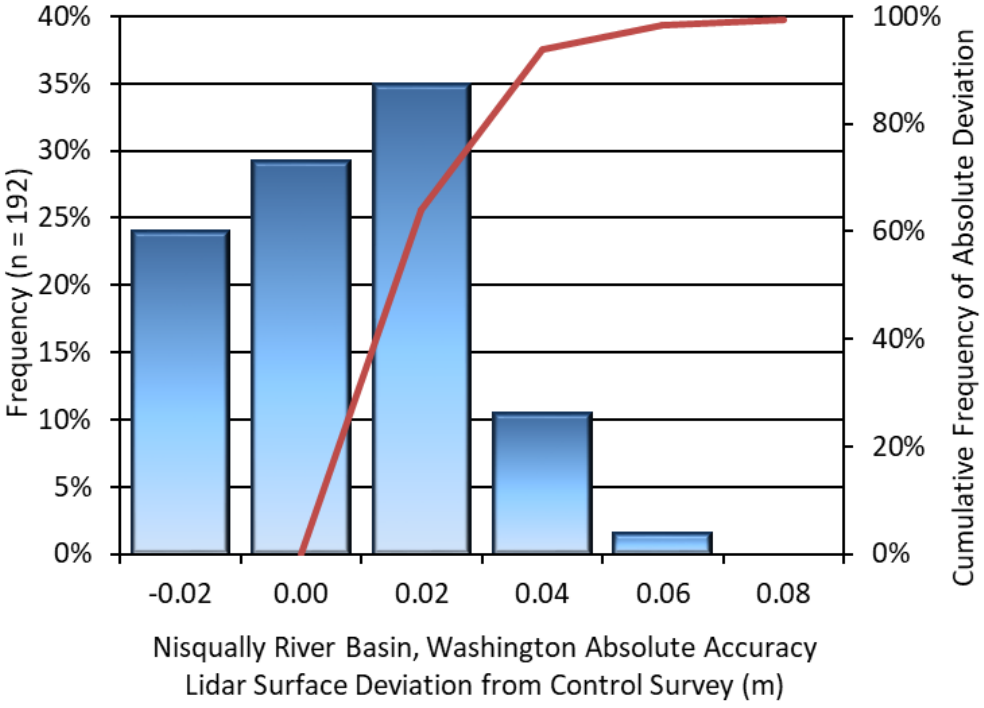

Figure 15: Frequency histogram for lidar surface deviation ground control point values

Lidar Bathymetric Vertical Accuracies

Submerged bathymetric as well as dry gravel bar check points were also collected in order to assess the riverine surface vertical accuracy. Assessment of 86 submerged bathymetric check points resulted in a vertical accuracy of 0.341 meters, while assessment of 15 gravel bar check points resulted in a vertical accuracy of 0.026 meters, evaluated at 95% confidence interval (Table 15, Figure 18).

Table 14: Bathymetric Vertical Accuracy for the Nisqually River Basin Project

Bathymetric Vertical Accuracy (BAP)		
	Submerged Bathymetric Check Points	**Gravel Bar Check Points**
Sample	86 points	15 points
95% Confidence (1.96*RMSE)	0.341 m	0.026 m
Average Dz	0.090 m	0.000 m
Median	0.030 m	-0.005 m
RMSE	0.174 m	0.013 m
Standard Deviation (1σ)	0.150 m	0.014 m

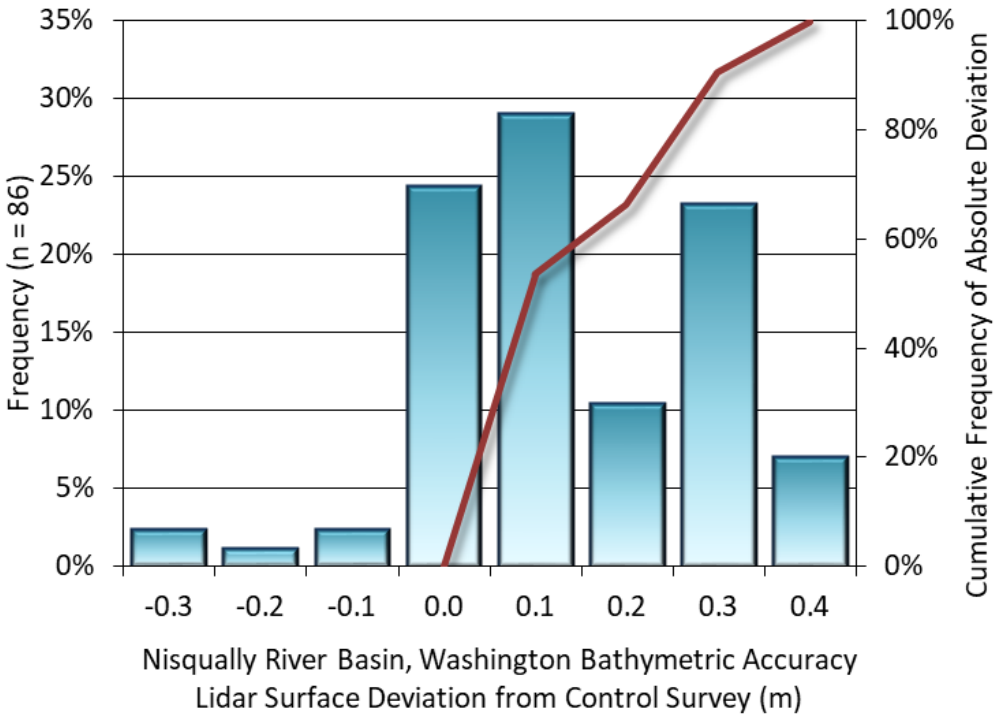

Figure 16: Frequency histogram for lidar surface deviation from submerged check point values

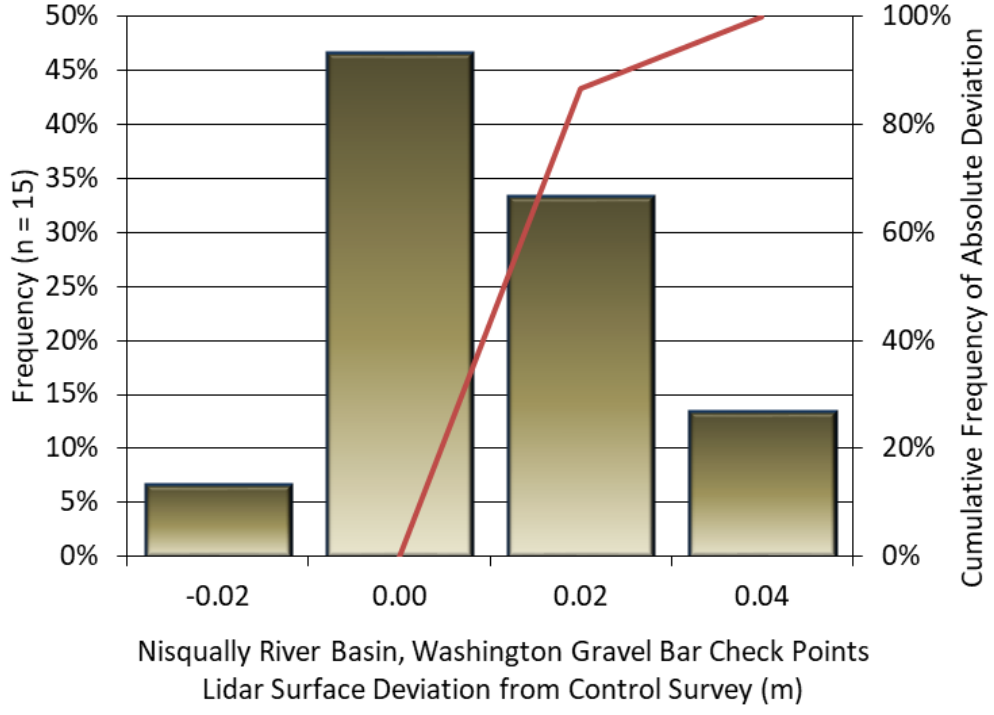

Figure 17: Frequency histogram for lidar surface deviation from gravel bar check point values

Lidar Vegetated Vertical Accuracies

NV5 also assessed vertical accuracy using Vegetated Vertical Accuracy (VVA) reporting. VVA compares known ground check point data collected over vegetated surfaces using land class descriptions to the DEM generated by the ground classified lidar points. VVA is evaluated at the 95th percentile (Table 15, Figure 18).

Table 15: Vegetated Vertical Accuracy for the Nisqually River Basin Project

Vegetated Vertical Accuracy (VVA)		
	NVA, as compared to Classified LAS	**NVA, as compared to Bare Earth DEM**
Sample	14 points	14 points
Average Dz	0.090 m	0.091 m
Median	0.084 m	0.086 m
RMSE	0.106 m	0.111 m
Standard Deviation (1σ)	0.058 m	0.065 m
95th Percentile	0.175 m	0.191 m

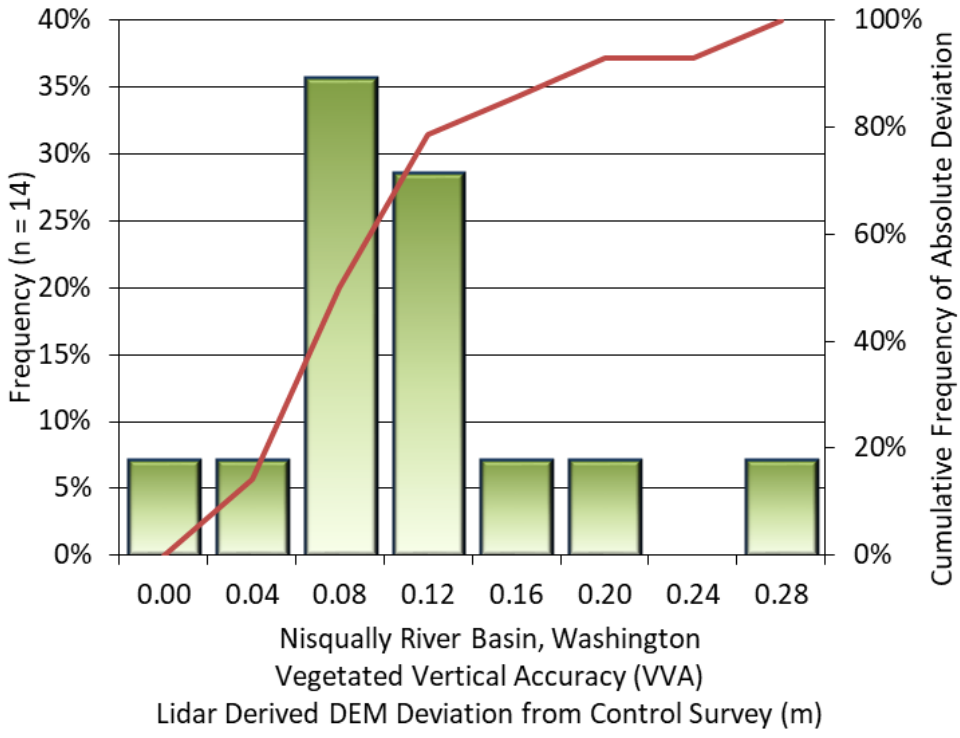

Figure 18: Frequency histogram for the DEM deviation from ground check point values from all land cover class point values (VVA)

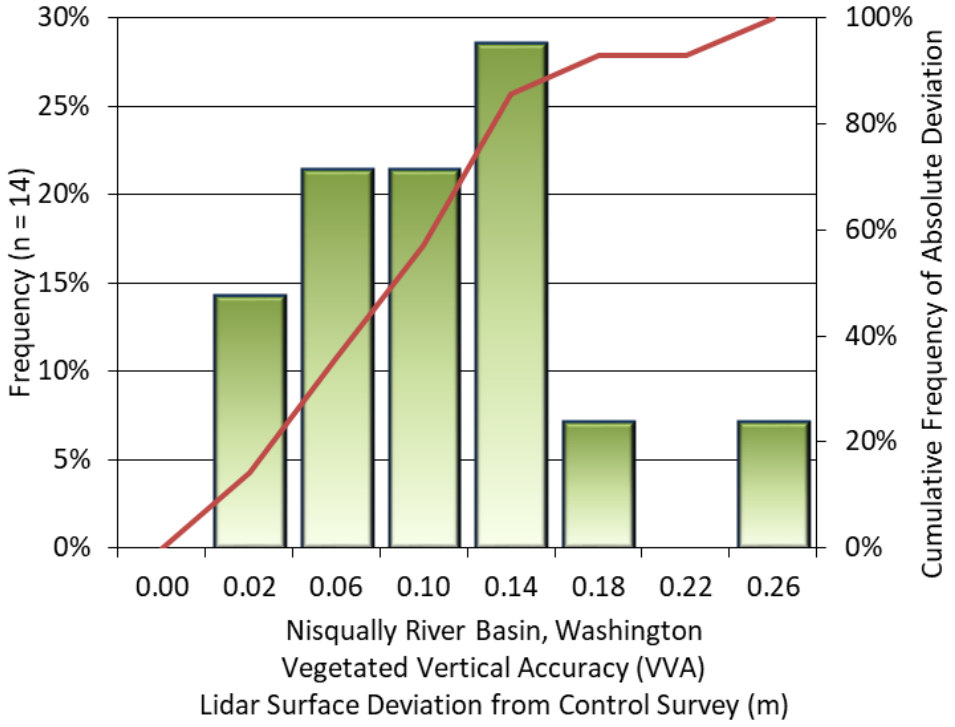

Figure 19: Frequency histogram for the lidar surface deviation from ground check point values from all land cover class point values (VVA)

Lidar Relative Vertical Accuracy

Relative vertical accuracy refers to the internal consistency of the data set as a whole: the ability to place an object in the same location given multiple flight lines, GPS conditions, and aircraft attitudes. When the lidar system is well calibrated, the swath-to-swath vertical divergence is low (<0.10 meters). The relative vertical accuracy was computed by comparing the ground surface model of each individual flight line with its neighbors in overlapping regions. The average (mean) line to line relative vertical accuracy for the Nisqually River Basin Lidar project was 0.048 meters (Table 16, Figure 20).

Table 16: Relative accuracy results

Relative Accuracy	
Sample	195 surfaces
Average	0.048 m
Median	0.044 m
RMSE	0.059 m
Standard Deviation (1σ)	0.028 m
1.96σ	0.055 m

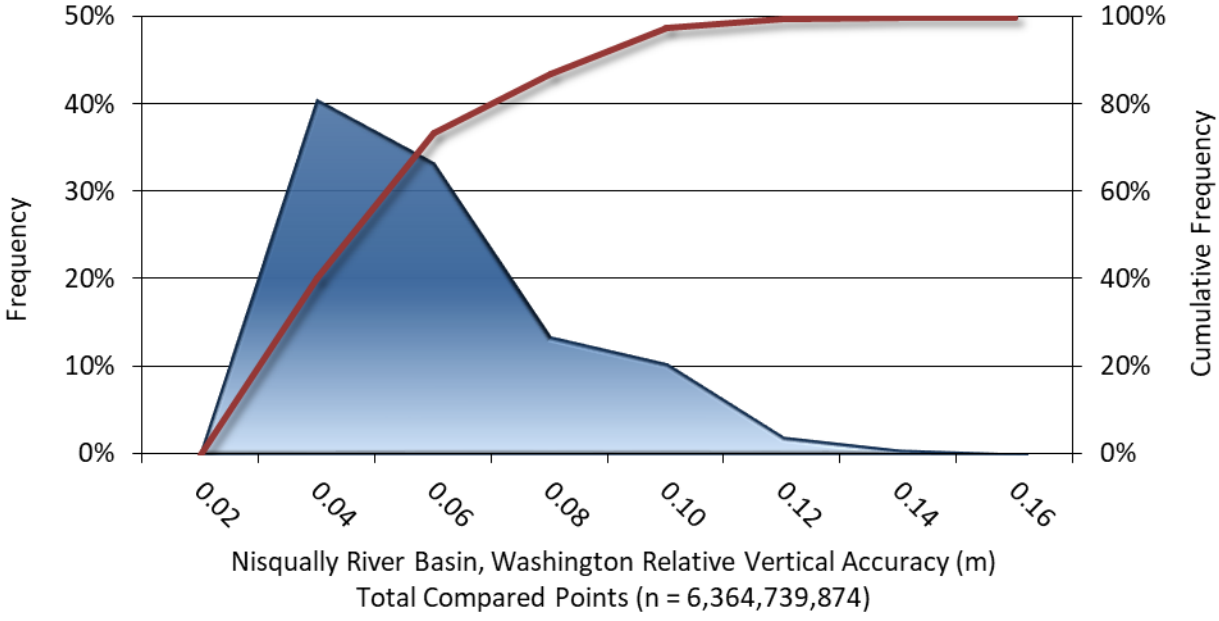

Figure 20: Frequency plot for relative vertical accuracy between flight lines

Lidar Horizontal Accuracy

Lidar horizontal accuracy is a function of Global Navigation Satellite System (GNSS) derived positional error, flying altitude, and INS derived attitude error. The obtained $RMSE_r$ value is multiplied by a conversion factor of 1.7308 to yield the horizontal component of the National Standards for Spatial Data Accuracy (NSSDA) reporting standard where a theoretical point will fall within the obtained radius 95 percent of the time. Based on a flying altitude of 400 meters, an IMU error of 0.002 decimal degrees, and a GNSS positional error of 0.015 meters, this project was compiled to meet 0.050 m horizontal accuracy at the 95% confidence level.

Table 17: Horizontal Accuracy

Horizontal Accuracy	
$RMSE_r$	0.029 m
ACC_r	0.050 m

CERTIFICATIONS

NV5 Geospatial, Inc. provided lidar services for the Nisqually River Basin project as described in this report.

I, Brian Von Seggern, have reviewed the attached report for completeness and hereby state that it is a complete and accurate report of this project.

Brian Von Seggern (Jul 16, 2021 14:43 PDT) Jul 16, 2021

Brian Von Seggern
Project Manager
NV5 Geospatial, Inc.

I, Evon P. Silvia, PLS, being duly registered as a Professional Land Surveyor in and by the state of Washington, hereby certify that the methodologies, static GNSS occupations used during airborne flights, and ground survey point collection were performed using commonly accepted Standard Practices. Field work conducted for this report was conducted between September 22 and December 22, 2020.

Accuracy statistics shown in the Accuracy Section of this Report have been reviewed by me and found to meet the "National Standard for Spatial Data Accuracy".

Evon P. Silvia Jul 16, 2021

Evon P. Silvia, PLS
NV5 Geospatial, Inc.
Corvallis, OR 97330

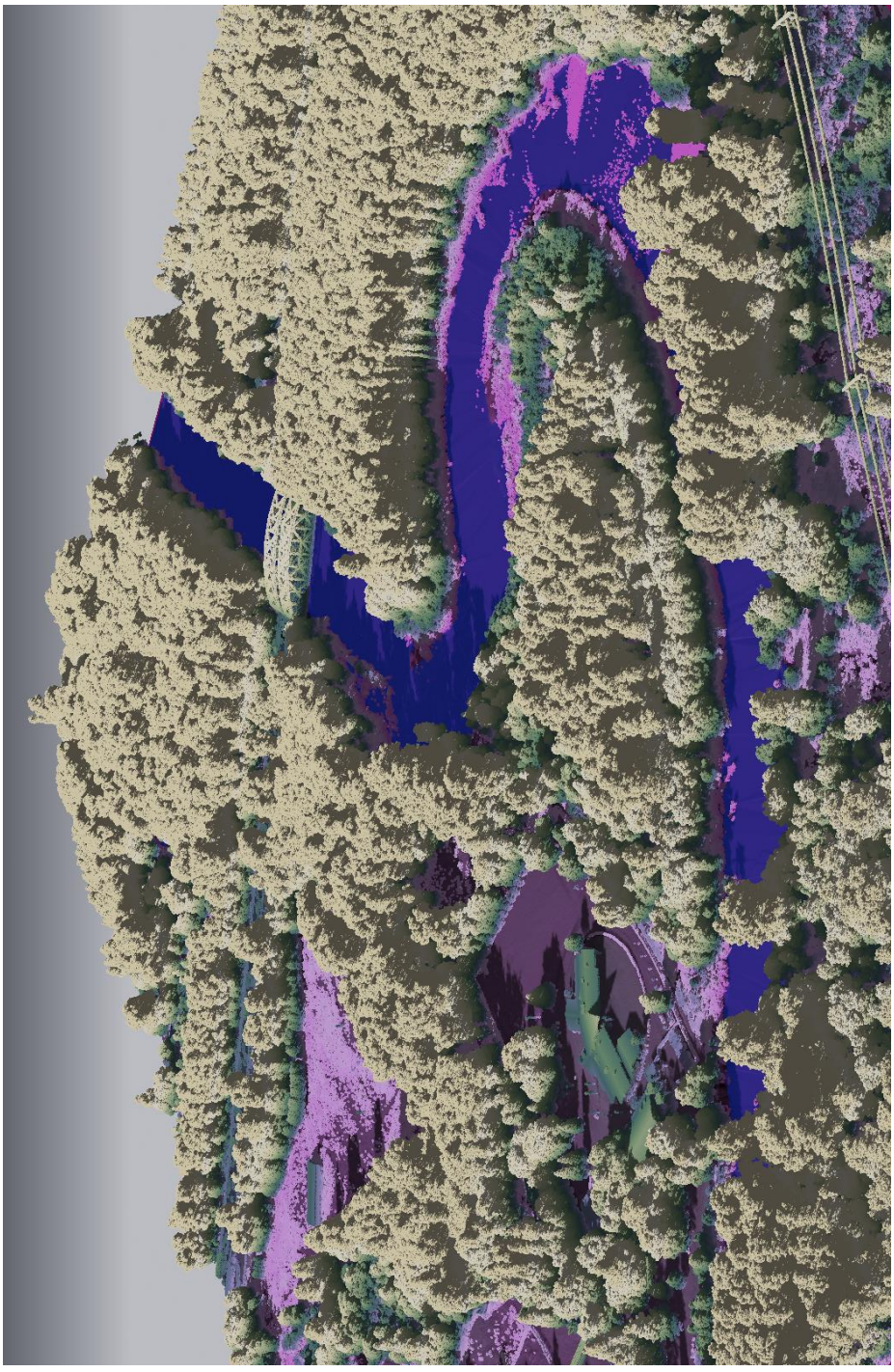

Figure 21: View looking north-west over the highway I-5 bridge crossing the Nisqually river. The image was created from the lidar bare earth model overlaid with the above-ground point cloud and colored by elevation.

GLOSSARY

1-sigma (σ) Absolute Deviation: Value for which the data are within one standard deviation (approximately 68th percentile) of a normally distributed data set.
1.96 * RMSE Absolute Deviation: Value for which the data are within two standard deviations (approximately 95th percentile) of a normally distributed data set, based on the FGDC standards for Non-vegetated Vertical Accuracy (FVA) reporting.
Accuracy: The statistical comparison between known (surveyed) points and laser points. Typically measured as the standard deviation (sigma σ) and root mean square error (RMSE).
Absolute Accuracy: The vertical accuracy of lidar data is described as the mean and standard deviation (sigma σ) of divergence of lidar point coordinates from ground survey point coordinates. To provide a sense of the model predictive power of the dataset, the root mean square error (RMSE) for vertical accuracy is also provided. These statistics assume the error distributions for x, y and z are normally distributed, and thus we also consider the skew and kurtosis of distributions when evaluating error statistics.
Relative Accuracy: Relative accuracy refers to the internal consistency of the data set; i.e., the ability to place a laser point in the same location over multiple flight lines, GPS conditions and aircraft attitudes. Affected by system attitude offsets, scale and GPS/IMU drift, internal consistency is measured as the divergence between points from different flight lines within an overlapping area. Divergence is most apparent when flight lines are opposing. When the lidar system is well calibrated, the line-to-line divergence is low (<10 cm).
Root Mean Square Error (RMSE): A statistic used to approximate the difference between real-world points and the lidar points. It is calculated by squaring all the values, then taking the average of the squares and taking the square root of the average.
Data Density: A common measure of lidar resolution, measured as points per square meter.
Digital Elevation Model (DEM): File or database made from surveyed points, containing elevation points over a contiguous area. Digital terrain models (DTM) and digital surface models (DSM) are types of DEMs. DTMs consist solely of the bare earth surface (ground points), while DSMs include information about all surfaces, including vegetation and man-made structures.
Intensity Values: The peak power ratio of the laser return to the emitted laser, calculated as a function of surface reflectivity.
Nadir: A single point or locus of points on the surface of the earth directly below a sensor as it progresses along its flight line.
Overlap: The area shared between flight lines, typically measured in percent. 100% overlap is essential to ensure complete coverage and reduce laser shadows.
Pulse Rate (PR): The rate at which laser pulses are emitted from the sensor; typically measured in thousands of pulses per second (kHz).
Pulse Returns: For every laser pulse emitted, the number of wave forms (i.e., echoes) reflected back to the sensor. Portions of the wave form that return first are the highest element in multi-tiered surfaces such as vegetation. Portions of the wave form that return last are the lowest element in multi-tiered surfaces.
Real-Time Kinematic (RTK) Survey: A type of surveying conducted with a GPS base station deployed over a known monument with a radio connection to a GPS rover. Both the base station and rover receive differential GPS data and the baseline correction is solved between the two. This type of ground survey is accurate to 1.5 cm or less.
Post-Processed Kinematic (PPK) Survey: GPS surveying is conducted with a GPS rover collecting concurrently with a GPS base station set up over a known monument. Differential corrections and precisions for the GNSS baselines are computed and applied after the fact during processing. This type of ground survey is accurate to 1.5 cm or less.
Scan Angle: The angle from nadir to the edge of the scan, measured in degrees. Laser point accuracy typically decreases as scan angles increase.
Native Lidar Density: The number of pulses emitted by the lidar system, commonly expressed as pulses per square meter.

Relative Accuracy Calibration Methodology:

Manual System Calibration: Calibration procedures for each mission require solving geometric relationships that relate measured swath-to-swath deviations to misalignments of system attitude parameters. Corrected scale, pitch, roll and heading offsets were calculated and applied to resolve misalignments. The raw divergence between lines was computed after the manual calibration was completed and reported for each survey area.

Automated Attitude Calibration: All data was tested and calibrated using TerraMatch automated sampling routines. Ground points were classified for each individual flight line and used for line-to-line testing. System misalignment offsets (pitch, roll and heading) and scale were solved for each individual mission and applied to respective mission datasets. The data from each mission were then blended when imported together to form the entire area of interest.

Automated Z Calibration: Ground points per line were used to calculate the vertical divergence between lines caused by vertical GPS drift. Automated Z calibration was the final step employed for relative accuracy calibration.

Lidar accuracy error sources and solutions:

Type of Error	Source	Post Processing Solution
GPS (Static/Kinematic)	Long Base Lines	None
	Poor Satellite Constellation	None
	Poor Antenna Visibility	Reduce Visibility Mask
Relative Accuracy	Poor System Calibration	Recalibrate IMU and sensor offsets/settings
	Inaccurate System	None
Laser Noise	Poor Laser Timing	None
	Poor Laser Reception	None
	Poor Laser Power	None
	Irregular Laser Shape	None

Operational measures taken to improve relative accuracy:

Low Flight Altitude: Terrain following was employed to maintain a constant above ground level (AGL). Laser horizontal errors are a function of flight altitude above ground (about 1/3000th AGL flight altitude).

Focus Laser Power at narrow beam footprint: A laser return must be received by the system above a power threshold to accurately record a measurement. The strength of the laser return (i.e., intensity) is a function of laser emission power, laser footprint, flight altitude and the reflectivity of the target. While surface reflectivity cannot be controlled, laser power can be increased and low flight altitudes can be maintained.

Reduced Scan Angle: Edge-of-scan data can become inaccurate. The scan angle was reduced to a maximum of ±20^{o} from nadir, creating a narrow swath width and greatly reducing laser shadows from trees and buildings.

Quality GPS: Flights took place during optimal GPS conditions (e.g., 6 or more satellites and PDOP [Position Dilution of Precision] less than 3.0). Before each flight, the PDOP was determined for the survey day. During all flight times, a dual frequency DGPS base station recording at 1 second epochs was utilized and a maximum baseline length between the aircraft and the control points was less than 13 nm at all times.

Ground Survey: Ground survey point accuracy (<1.5 cm RMSE) occurs during optimal PDOP ranges and targets a minimal baseline distance of 4 miles between GPS rover and base. Robust statistics are, in part, a function of sample size (n) and distribution. Ground survey points are distributed to the extent possible throughout multiple flight lines and across the survey area.

50% Side-Lap (100% Overlap): Overlapping areas are optimized for relative accuracy testing. Laser shadowing is minimized to help increase target acquisition from multiple scan angles. Ideally, with a 50% side-lap, the nadir portion of one flight line coincides with the swath edge portion of overlapping flight lines. A minimum of 50% side-lap with terrain-followed acquisition prevents data gaps.

Opposing Flight Lines: All overlapping flight lines have opposing directions. Pitch, roll and heading errors are amplified by a factor of two relative to the adjacent flight line(s), making misalignments easier to detect and resolve.